Correlations among New Dental and Cranial Measurements

DENTAL ANTHROPOLOGY

Volume 29, Issue 01, 2016 ISSN 1096-9411

doctor **Massimo Scioletti** / dental-orthopedic technician **Dino Scioletti**
engineer **Andrea Ferrara** / doctor **Salvatore Dettori** / doctor **Roberto Carboni**
doctor **Dario Stefani** / doctor **Rosalba Floris**
doctor **Ruggero D'Anastasio** / doctor **Joan Viciano**

The aim of this article is to propose new craniometric and dental landmarks and inter-landmark distances that may have important applications in Dentistry and Phisical Anthropology

doctor **Massimo Scioletti** | dental-orthopedic technician **Dino Scioletti** | engineer **Andrea Ferrara**

Dental clinic “San Francesco”, via Mons. Tesauri 10, 66034 Lanciano, Italy
posturasm@gmail.com

doctor **Salvatore Dettori** | doctor **Roberto Carboni**

Dental clinic “Dettori”, via Donizetti 13, 07037 Sorso, Italy | gnatologia@tiscali.it

doctor **Dario Stefani**

Dental clinic “Stefani”, viale Colombo 87, 09045 Quartu Sant’Elena, Italy

doctor **Rosalba Floris**

Department of Life Sciences and Environment, State University of Cagliari,
Cittadella Universitaria, S.S. 554 - km 4,500, 09042 Monserrato, Italy

doctor **Ruggero D’Anastasio** | doctor **Joan Viciano**

University Museum, “G. d’Annunzio” University of Chieti-Pescara,
Piazza Trento e Trieste 1, 66100 Chieti, Italy
Department of Medicine and Aging Science, “G. d’Annunzio” University of Chieti-Pescara
Via dei Vestini, 66013 Chieti Scalo, Italy

Materials and methods

The anthropometric and dental measurments were taken on 30 middle ages adult crania from Sardinia (Italy).

Data acquisition and analysis

A MicroScribe portable digitizer (Model MX, Immersion Corporation, San Jose, CA, USA) and the integrated MicroScribe Utility Software were used to collect the data for the distances between the anatomical landmarks with an accuracy of 0.05 mm.

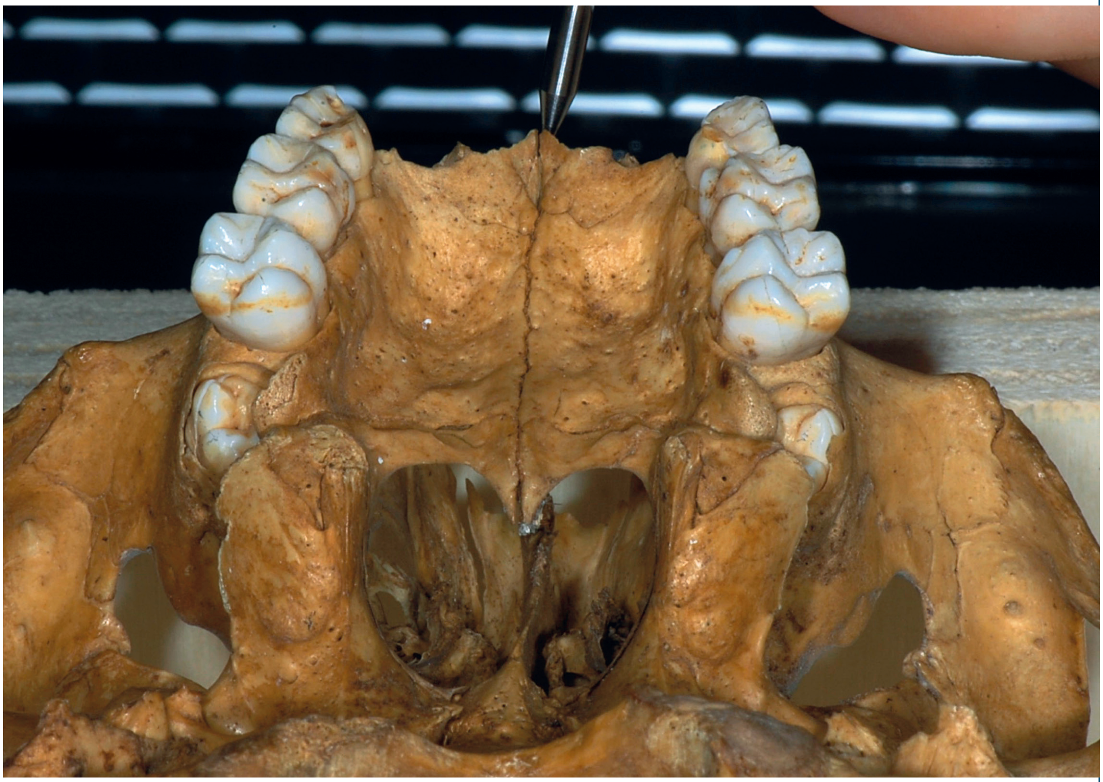

The purpose of this article is to propose new craniometric and dental reference points that have significant statistical correlation with anthropometric points used in classical anthropology

n. - s. - ba. - op. - pr. - sta.

Reference points

New points of reference represent anatomical points of muscle insertion, direct dental points and dental points

pht, bms, stl , gfb, zig, D4, D5, D6, D7

on geometric construction

pT4, pT5, pT6, pT7

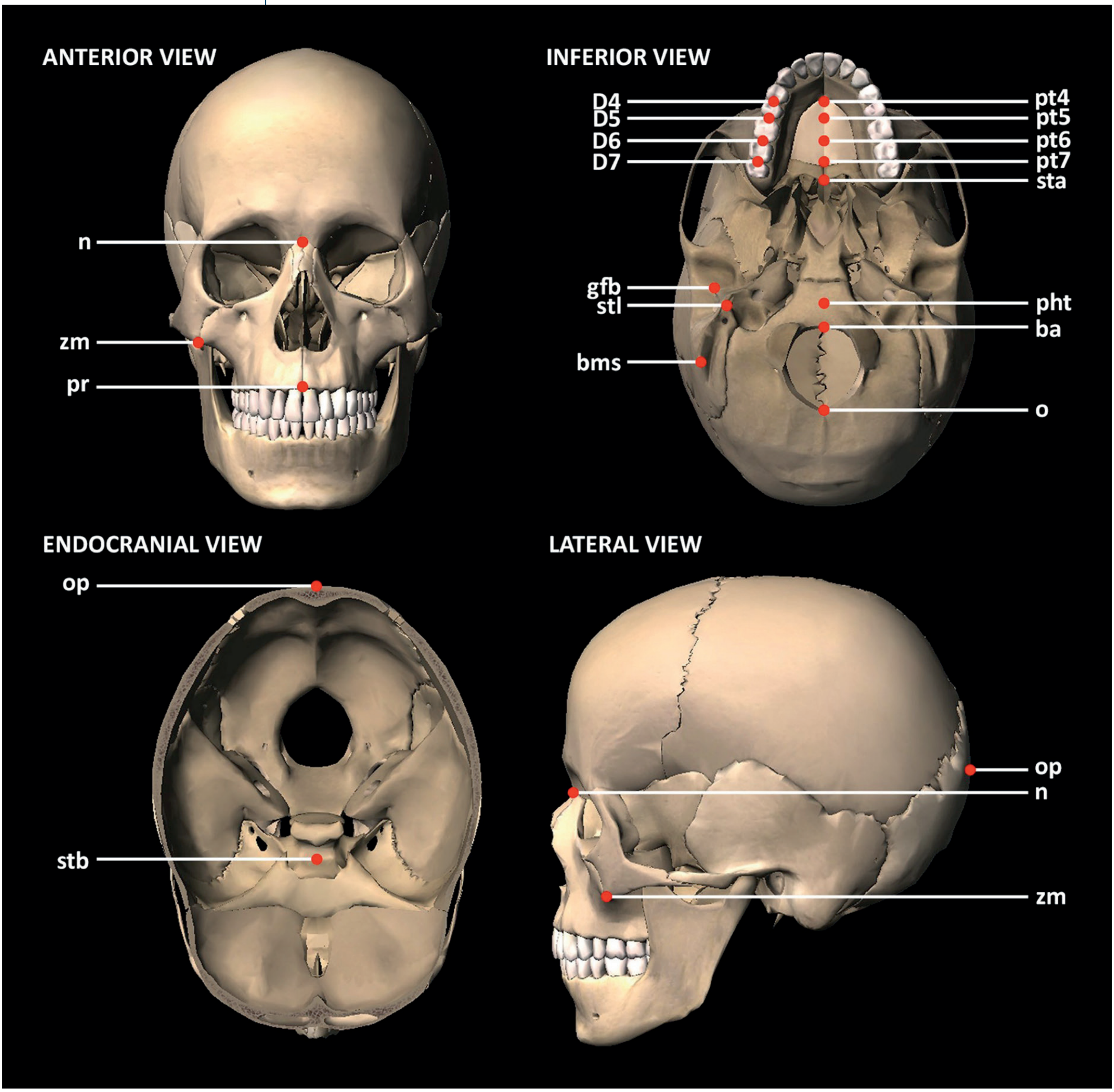

THE LANDMARKS WERE DIVIDED INTO THREE ANATOMICAL REGIONS:

- (i) **the oral cavity**, which included the pr, sta, D4, D5, D6, D7, pt4, pt5, pt6 and pt7 landmarks;
- (ii) **the base of the cranium**, which included the pht, ba, o, gfb, stl and bms landmarks;
- (iii) **the upper cranium**, which included n, stb, zm and op landmarks (see Table 1 and Figure 1).

TABLE 1. Description of landmarks used in this study

Anatomical region	Source	Landmark	Location	Code	Definition
Oral cavity	Direct acquisition	Prosthion[a]	Midline	pr	Most anterior point on the alveolar process between the two upper central incisors, in the midsagittal plane
		Staphilion[a]	Midline	sta	The point on the posterior hard palate where the palatal suture is crossed by a line drawn tangent to the curves of the posterior margin of the palatal bones
		Distal surface first premolar[b]	Bilateral	D4	Most occluso-distal point of the crown
		Distal surface second premolar[b]	Bilateral	D5	Most occluso-distal point of the crown
		Distal surface first molar[b]	Bilateral	D6	Most occluso-distal point of the crown
		Distal surface second molar[b]	Bilateral	D7	Most occluso-distal point of the crown
	Calculated landmarks	Point 4[b]	Midline	pt4	Midpoint of the distance between the distal points of the first premolars
		Point 5[b]	Midline	pt5	Midpoint of the distance between the distal points of the second premolars
		Point 6[b]	Midline	pt6	Midpoint of the distance between the distal points of the first molars
		Point 7[b]	Midline	pt7	Midpoint of the distance between the distal points of the second molars
Base of the cranium	Direct acquisition	Pharyngeal tubercle[b]	Midline	pht	Bone tubercle on the lower surface of the basilar part of occipital bone, about 1 cm. anterior to the *foramen magnum*, which gives attachment to the fibrous raphe of the pharynx
		Basion[a]	Midline	ba	Point on the anterior margin of the *foramen magnum* in the midsagittal plane.
		Opisthion[a]	Midline	o	Most posterior point on the posterior margin of the *foramen magnum* in the midsagittal plane
		Base of the glenoid fossa[b]	Bilateral	gfb	The more medial and caudal point of the glenoid fossa
		Styloid process[b]	Bilateral	stl	Posterior point of the base of the styloid process
		Base of mastoid process[b]	Bilateral	bms	Posterior point of the base of mastoid process
Upper cranium	Direct acquisition	Nasion[a]	Midline	n	Point at junction of internasal suture and nasofrontal suture, in midsaggital plane
		Base of sella turcica[a]	Midline	stb	The midpoint of the hypophyseal fossa
		Zygomaxillare[a]	Bilateral	zm	Point located externally at the lowest extent of the zygomaticomaxillary suture
		Opisthocranion[a]	Midline	op	Instrumentally determined point marking maximum skull length, as measured from glabella. This point is in the midsagittal plane

[a] Landmarks described by Martin and Knußmann (1988).
[b] Modified definitions from Martin and Knußmann (1988) or new landmarks used in the current study.

Subsequently, a series of **62 virtual triangles** were also constructed that had at least the central vertex located on the mid-line of the skull or maxilla (Figure 2). Principal components analysis was performed to explore the correlations among inter-landmark distances.

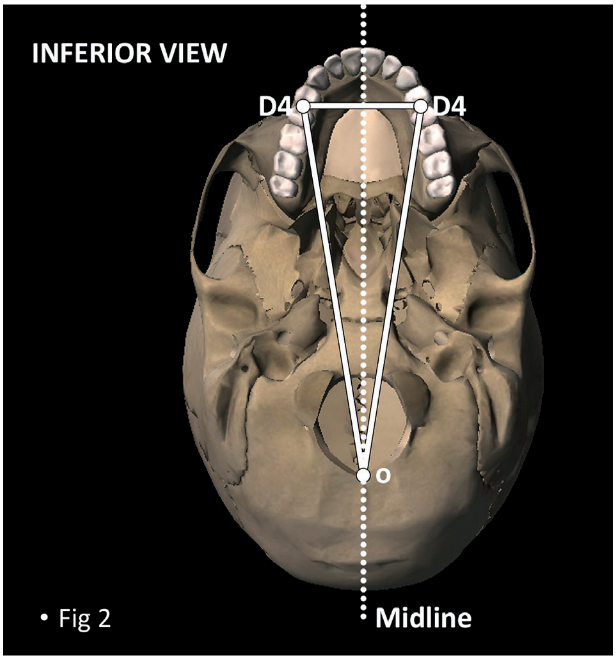

• Fig 2

TABLE 2. Descriptive statistics of inter-landmark distances

Triangle	Inter-landmark distance	N	Minimum	Maximum	Mean	SD
D4 – op – D4	D4 – D4	30	36.28	44.92	39.432	2.015
	op – D4	30	163.92	197.865	180.923	7.989
D4 – o – D4	D4 – D4	30	36.28	44.92	39.432	2.015
	o – D4	30	103.24	128.505	115.071	6.289
D4 – ba – D4	D4 – D4	30	36.28	44.92	39.432	2.015
	ba – D4	29	72.285	88.895	82.475	4.753
D4 – n – D4	D4 – D4	30	36.28	44.92	39.432	2.015
	n – D4	30	65.295	84.675	75.557	5.122
D4 – pr – D4	D4 – D4	30	36.28	44.92	39.432	2.015
	pr – D4	28	24.71	31.235	27.407	1.678
D4 – sta – D4	D4 – D4	30	36.28	44.92	39.432	2.015
	sta – D4	28	40.13	47.88	43.701	2.12
D4 – pht – D4	D4 – D4	30	36.28	44.92	39.432	2.015
	pht – D4	29	67.4	81.695	75.378	3.847
D4 – stb – D4	D4 – D4	30	36.28	44.92	39.432	2.015
	stb – D4	30	71.915	84.265	78.653	3.664
D4 – pt6 – D4	D4 – D4	30	36.28	44.92	39.432	2.015
	pt6 – D4	30	22.95	28.39	25.66	1.31
D5 – op – D5	D5 – D5	30	37.3	52.23	43.126	3.34
	op – D5	30	160.52	197.09	176.646	8.237
D5 – o – D5	D5 – D5	30	37.3	52.23	43.126	3.34
	o – D5	29	98.275	122.63	109.509	5.983
D5 – ba – D5	D5 – D5	30	37.3	52.23	43.126	3.34
	ba – D5	29	68.43	86.74	78.101	4.785
D5 – n – D5	D5 – D5	30	37.3	52.23	43.126	3.34
	n – D5	30	70.26	88.395	79.087	4.966
D5 – pr – D5	D5 – D5	30	37.3	52.23	43.126	3.34
	pr – D5	29	29	37.035	33.022	1.896
D5 – sta – D5	D5 – D5	30	37.3	52.23	43.126	3.34
	sta – D5	28	38.415	46.115	40.953	2.082
D5 – pht – D5	D5 – D5	30	37.3	52.23	43.126	3.34
	pht – D5	29	64.505	79.67	71.493	3.816

Triangle	Inter-landmark distance	N	Minimum	Maximum	Mean	SD
D5 – stb – D5	D5 – D5	30	37.3	52.23	43.126	3.34
	stb – D5	30	67.265	86.195	76.724	3.627
D5 – pt4 – D5	D5 – D5	30	37.3	52.23	43.126	3.34
	pt4 – D5	30	19.21	26.61	22.685	1.732
D5 – pt6 – D5	D5 – D5	30	37.3	52.23	43.126	3.34
	pt6 – D5	30	20.75	28.375	23.824	1.746
D6 – op – D6	D6 – D6	30	44.37	57.56	49.66	2.841
	op – D6	30	153.525	189.135	168.369	8.257
D6 – o – D6	D6 – D6	30	44.37	57.56	49.66	2.841
	o – D6	29	90.735	114.67	100.758	6.154
D6 – ba – D6	D6 – D6	30	44.37	57.56	49.66	2.841
	ba – D6	30	62.055	80.225	70.731	5.204
D6 – n – D6	D6 – D6	30	44.37	57.56	49.66	2.841
	n – D6	30	74.405	94.35	83.014	4.727
D6 – pr – D6	D6 – D6	30	44.37	57.56	49.66	2.841
	pr – D6	29	38.23	46.325	42.476	1.963
D6 – sta – D6	D6 – D6	30	44.37	57.56	49.66	2.841
	sta – D6	29	33.14	40.735	36.907	1.755
D6 – pht – D6	D6 – D6	30	44.37	57.56	49.66	2.841
	pht – D6	29	57.19	73.695	64.491	4.067
D6 – stb – D6	D6 – D6	30	44.37	57.56	49.66	2.841
	stb – D6	30	65.27	83.66	72.358	3.795
D6 – pt4 – D6	D6 – D6	30	44.37	57.56	49.66	2.841
	pt4 – D6	30	26.1	33.615	29.77	1.617
D7 – op – D7	D7 – D7	30	45.9	60.54	52.994	3.044
	op – D7	30	145.725	179.07	160.094	8.051
D7 – o – D7	D7 – D7	30	45.9	60.54	52.994	3.044
	o – D7	29	82.235	105.79	92.806	5.969
D7 – ba – D7	D7 – D7	30	45.9	60.54	52.994	3.044
	ba – D7	30	53.32	72.83	63.315	5.147
D7 – n – D7	D7 – D7	30	45.9	60.54	52.994	3.044
	n – D7	30	73.645	96.69	84.384	5.154

TABLE 2. Descriptive statistics of inter-landmark distances, cont'd

Triangle	Inter-landmark distance	N	Minimum	Maximum	Mean	SD
D7 – pr – D7	D7 – D7	30	45.9	60.54	52.994	3.044
	pr – D7	29	45.53	53.895	49.778	2.196
D7 – sta – D7	D7 – D7	30	45.9	60.54	52.994	3.044
	sta – D7	28	25.99	37.68	33.313	2.281
D7 – pht – D7	D7 – D7	30	45.9	60.54	52.994	3.044
	pht – D7	29	47.46	65.59	57.455	4.238
D7 – stb – D7	D7 – D7	30	45.9	60.54	52.994	3.044
	stb – D7	30	57.04	78.035	66.932	4.115
D7 – pt4 – D7	D7 – D7	30	45.9	60.54	52.994	3.044
	pt4 – D7	30	32.765	41	36.169	1.89
D7 – pt6 – D7	D7 – D7	30	45.9	60.54	52.994	3.044
	pt6 – D7	30	25.57	31.495	27.99	1.443
zm – pr – zm	zm – zm	30	83.66	124.93	95.985	7.478
	pr – zm	30	51.791	78.83	58.854	5.456
zm – pt4 – zm	zm – zm	30	83.66	124.93	95.985	7.478
	pt4 – zm	30	47.208	72.99	54.61	5.204
zm – pt5 – zm	zm – zm	30	83.66	124.93	95.985	7.478
	pt5 – zm	30	48.233	72.38	54.425	4.895
zm – pt6 – zm	zm – zm	30	83.66	124.93	95.985	7.478
	pt6 – zm	30	48.193	70.998	54.239	4.442
zm – pt7 – zm	zm – zm	30	83.66	124.93	95.985	7.478
	pt7 – zm	30	47.755	69.667	54.283	4.051
zm – sta – zm	zm – zm	30	83.66	124.93	95.985	7.478
	sta – zm	30	48.284	64.307	53.373	3.08
gfb – pr – gfb	gfb – gfb	30	81.02	98.37	90.007	5.126
	pr – gfb	30	90.305	106.91	99.063	4.057
gfb – pt4 – gfb	gfb – gfb	30	81.02	98.37	90.007	5.126
	pt4 – gfb	30	79.67	96.359	88.442	3.824
gfb – pt5 – gfb	gfb – gfb	30	81.02	98.37	90.007	5.126
	pt5 – gfb	30	77.783	92.833	85.235	3.655

Triangle	Inter-landmark distance	N	Minimum	Maximum	Mean	SD
gfb – pt6 – gfb	gfb – gfb	30	81.02	98.37	90.007	5.126
	pt6 – gfb	30	72.338	86.557	78.967	3.702
gfb – pt7 – gfb	gfb – gfb	30	81.02	98.37	90.007	5.126
	pt7 – gfb	30	64.986	80.248	72.662	3.682
gfb – sta – gfb	gfb – gfb	30	81.02	98.37	90.007	5.126
	sta – gfb	30	52.848	96.005	59.842	7.346
stl – pr – stl	stl – stl	30	61.18	82.92	73.589	5.822
	pr – stl	30	87.066	110.219	96.866	5.465
stl – pt4 – stl	stl – stl	30	61.18	82.92	73.589	5.822
	pt4 – stl	30	71.497	95.088	82.623	6.019
stl – pt5 – stl	stl – stl	30	61.18	82.92	73.589	5.822
	pt5 – stl	30	66.62	90.169	78.031	6.028
stl – pt6 – stl	stl – stl	30	61.18	82.92	73.589	5.822
	pt6 – stl	30	57.788	82.064	69.951	5.952
stl – pt7 – stl	stl – stl	30	61.18	82.92	73.589	5.822
	pt7 – stl	30	50.497	74.686	62.674	5.75
stl – sta – stl	stl – stl	30	61.18	82.92	73.589	5.822
	sta – stl	30	43.62	83.549	53.431	7.002
bms – pr – bms	bms – bms	30	90.67	109.89	98.825	3.941
	pr – bms	30	104.919	125.308	114.227	5.088
bms – pt4 – bms	bms – bms	30	90.67	109.89	98.825	3.941
	pt4 – bms	30	91.216	108.945	99.601	4.827
bms – pt5 – bms	bms – bms	30	90.67	109.89	98.825	3.941
	pt5 – bms	30	86.896	104.009	94.804	4.8
bms – pt6 – bms	bms – bms	30	90.67	109.89	98.825	3.941
	pt6 – bms	30	79.231	95.879	86.658	4.76
bms – pt7 – bms	bms – bms	30	90.67	109.89	98.825	3.941
	pt7 – bms	30	72.511	88.059	79.636	4.497
bms – sta – bms	bms – bms	30	90.67	109.89	98.825	3.941
	sta – bms	30	62.802	106.875	72.287	7.39

Dental Anthropology

2016 | Volume 29 | Issue 01

Result

Principal component analysis returned ten components that explained **94.6%** of the variation. Here, only the first three components were considered to facilitate the interpretation of the data, and these explained **67.1%** of the variation in the data set.
The loadings of the original variables on these *three* rotated principal components are illustrated in Tab 3.

TABLE 3. Ten components of the principal components analysis of the interlandmark distances

Principal component	Eigenvalue	Explained variance (%)	Cumulative variance (%)
PC1	30.052	42.932	42.932
PC2	9.137	13.052	55.985
PC3	7.792	11.131	67.116
PC4	5.432	7.759	74.875
PC5	3.723	5.319	80.194
PC6	3.346	4.779	84.973
PC7	2.233	3.190	88.163
PC8	1.993	2.847	91.010
PC9	1.370	1.957	92.967
PC10	1.159	1.655	94.623

TABLE 4. Bivariate product-moment correlations for inter-landmark distances included in PC1

	o-D4	ba-D4	pht-D4	o-D5	ba-D5	pht-D5	o-D6	ba-D6	pht-D6	o-D7	ba-D7	pht-D7	pr-gfb	pt4-gfb	pt5-gfb	pt6-gfb	pt7-gfb	sta-gfb	pr-bma	pt4-bma	pt5-bma	pt6-bma	pt7-bma
o-D4	–																						
ba-D4	0.883	–																					
pht-D4	0.839	0.940	–																				
o-D5	0.988	0.876	0.837	–																			
ba-D5	0.865	0.978	0.920	0.887	–																		
pht-D5	0.808	0.902	0.958	0.841	0.942	–																	
o-D6	0.971	0.852	0.812	0.986	0.862	0.811	–																
ba-D6	0.869	0.947	0.894	0.879	0.974	0.914	0.892	–															
pht-D6	0.786	0.866	0.918	0.827	0.910	0.957	0.845	0.948	–														
o-D7	0.965	0.832	0.809	0.969	0.829	0.787	0.988	0.864	0.828	–													
ba-D7	0.867	0.932	0.900	0.865	0.942	0.898	0.887	0.983	0.946	0.887	–												
pht-D7	0.764	0.829	0.900	0.790	0.853	0.910	0.819	0.906	0.971	0.833	0.950	–											
pr-gfb	0.795	0.832	0.804	0.789	0.853	0.815	0.764	0.847	0.780	0.734	0.817	0.718	–										
pt4-gfb	0.711	0.765	0.774	0.666	0.762	0.754	0.609	0.734	0.668	0.577	0.704	0.607	0.862	–									
pt5-gfb	0.655	0.675	0.678	0.636	0.734	0.756	0.576	0.711	0.669	0.529	0.664	0.584	0.835	0.939	–								
pt6-gfb	0.684	0.694	0.705	0.675	0.750	0.765	0.665	0.784	0.766	0.631	0.758	0.708	0.852	0.912	0.954	–							
pt7-gfb	0.715	0.718	0.736	0.690	0.746	0.752	0.695	0.797	0.774	0.690	0.809	0.773	0.839	0.886	0.889	0.967	–						
sta-gfb	0.247	0.374	0.385	0.338	0.505	0.548	0.318	0.491	0.548	0.258	0.437	0.467	0.538	0.517	0.652	0.649	0.556	–					
pr-bma	0.847	0.859	0.845	0.838	0.861	0.834	0.812	0.848	0.787	0.795	0.831	0.741	0.894	0.773	0.721	0.736	0.753	0.286	–				
pt4-bma	0.822	0.836	0.830	0.797	0.833	0.822	0.762	0.811	0.756	0.746	0.793	0.707	0.785	0.808	0.767	0.758	0.753	0.246	0.931	–			
pt5-bma	0.795	0.801	0.802	0.794	0.832	0.834	0.765	0.820	0.783	0.739	0.792	0.719	0.789	0.786	0.779	0.780	0.761	0.322	0.931	0.985	–		
pt6-bma	0.792	0.780	0.780	0.793	0.809	0.803	0.795	0.835	0.804	0.776	0.817	0.755	0.767	0.740	0.726	0.777	0.773	0.289	0.916	0.963	0.984	–	
pt7-bma	0.777	0.754	0.766	0.766	0.765	0.764	0.771	0.800	0.768	0.778	0.806	0.749	0.736	0.710	0.676	0.737	0.765	0.214	0.906	0.951	0.964	0.986	–
sta-bma	0.376	0.503	0.521	0.466	0.634	0.682	0.446	0.619	0.677	0.391	0.568	0.596	0.616	0.564	0.683	0.683	0.593	0.953	0.462	0.438	0.514	0.484	0.415

Significant correlations ($p < 0.05$) are in bold.

The "cranial base system"

The first component (PC1- 42.9%) showed correlations between the cranial base and maxillary inter-landmark distances.

The loadings of the distances that include the **o, ba, pht** midline landmarks with all of the dental bilateral landmarks (**D4, D5, D6** and **D7**) are slightly higher than the others. (Tab 4a)

PC 1

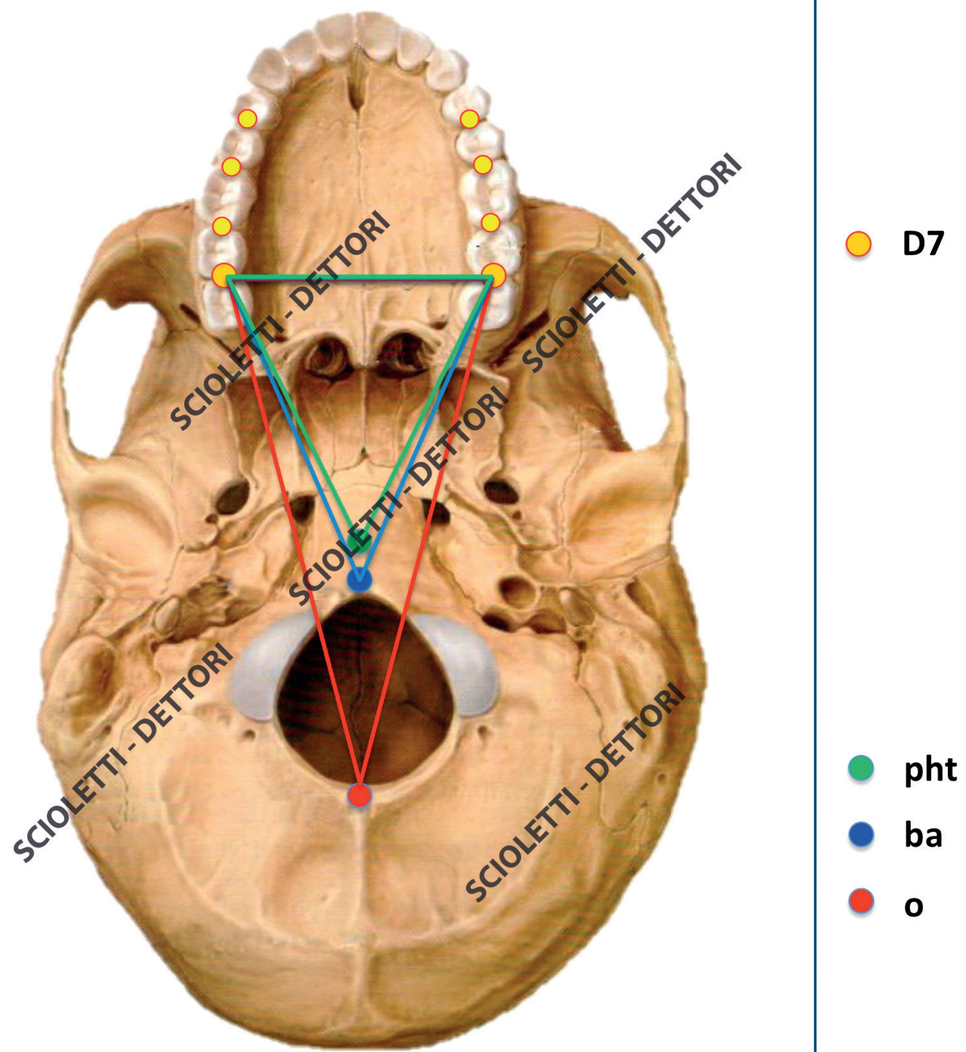

Tabella 4a

THE "CRANIAL BASE SYSTEM"

Also, the distances that include the **pr, pt4, pt5, pt6, pt7** and ***sta*** maxillary midline landmarks with the **gfb** and **bms** bilateral landmarks show high shared variance for PC1. (Tab 4b)

TABLE 4. Bivariate product-moment correlations for inter-landmark distances included in PC1

	o-D4	ba-D4	pht-D4	o-D5	ba-D5	pht-D5	o-D6	ba-D6	pht-D6	o-D7	ba-D7	pht-D7	pr-gfb	pt4-gfb	pt5-gfb	pt6-gfb	pt7-gfb	sta-gfb	pr-bms	pt4-bms	pt5-bms	pt6-bms	pt7-bms
o-D4	–																						
ba-D4	0.883	–																					
pht-D4	0.839	0.940	–																				
o-D5	0.988	0.876	0.837	–																			
ba-D5	0.865	0.978	0.920	0.887	–																		
pht-D5	0.808	0.902	0.958	0.841	0.942	–																	
o-D6	0.971	0.852	0.812	0.986	0.862	0.811	–																
ba-D6	0.869	0.947	0.894	0.879	0.974	0.914	0.892	–															
pht-D6	0.786	0.866	0.918	0.827	0.910	0.957	0.845	0.948	–														
o-D7	0.965	0.832	0.809	0.969	0.829	0.787	0.988	0.864	0.828	–													
ba-D7	0.867	0.932	0.900	0.865	0.942	0.898	0.887	0.983	0.946	0.887	–												
pht-D7	0.764	0.829	0.900	0.790	0.853	0.910	0.819	0.906	0.971	0.833	0.950	–											
pr-gfb	0.795	0.832	0.804	0.789	0.853	0.815	0.764	0.847	0.780	0.734	0.817	0.718	–										
pt4-gfb	0.711	0.765	0.774	0.666	0.762	0.754	0.609	0.734	0.668	0.577	0.704	0.607	0.862	–									
pt5-gfb	0.655	0.675	0.678	0.636	0.734	0.756	0.576	0.711	0.669	0.529	0.664	0.584	0.835	0.939	–								
pt6-gfb	0.684	0.694	0.705	0.675	0.750	0.765	0.665	0.784	0.766	0.631	0.758	0.708	0.852	0.912	0.954	–							
pt7-gfb	0.715	0.718	0.736	0.690	0.746	0.752	0.695	0.797	0.774	0.690	0.809	0.773	0.839	0.886	0.889	0.967	–						
sta-gfb	0.247	0.374	0.385	0.338	0.505	0.548	0.318	0.491	0.548	0.258	0.437	0.467	0.538	0.517	0.652	0.649	0.556	–					
pr-bms	0.847	0.859	0.845	0.838	0.861	0.834	0.812	0.848	0.787	0.795	0.831	0.741	0.894	0.773	0.721	0.736	0.753	0.286	–				
pt4-bms	0.822	0.836	0.830	0.797	0.833	0.822	0.762	0.811	0.756	0.746	0.793	0.707	0.785	0.808	0.767	0.758	0.753	0.246	0.931	–			
pt5-bms	0.795	0.801	0.802	0.794	0.832	0.834	0.765	0.820	0.783	0.739	0.792	0.719	0.789	0.786	0.779	0.780	0.761	0.322	0.931	0.985	–		
pt6-bms	0.792	0.780	0.780	0.793	0.809	0.803	0.795	0.835	0.804	0.776	0.817	0.755	0.767	0.740	0.726	0.777	0.773	0.289	0.916	0.963	0.984	–	
pt7-bms	0.777	0.754	0.766	0.766	0.765	0.764	0.771	0.800	0.768	0.778	0.806	0.749	0.736	0.710	0.676	0.737	0.765	0.214	0.906	0.951	0.964	0.986	–
sta-bms	0.376	0.503	0.521	0.466	0.634	0.682	0.446	0.619	0.677	0.391	0.568	0.596	0.616	0.564	0.683	0.683	0.593	0.953	0.462	0.438	0.514	0.484	0.415

Significant correlations ($p < 0.05$) are in bold.

THE "CRANIAL BASE SYSTEM"

The **PC1** shows correlations between the cranial base and the maxillary distances.

The landmarks of the cranial base system refer to muscle insertions, articular joints, and vascular and neuronal areas.

PC 1

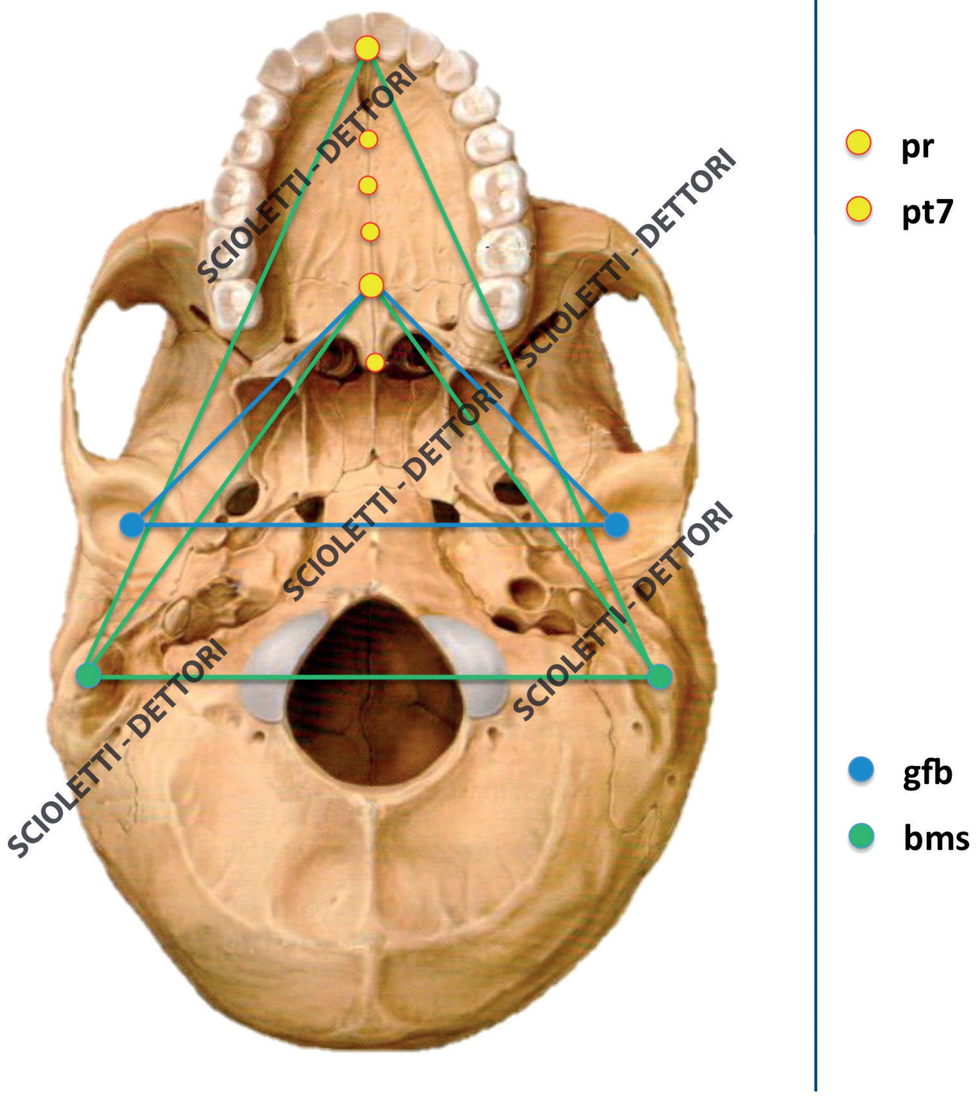

Tabella 4b

THE "ORAL CAVITY SYSTEM"

The second component (PC2 - **13.05%**) exclusively demonstrated correlations among maxillary and dental inter-landmark distances (the "oral cavity system"). (Tab 5)

TABLE 5. Bivariate product-moment correlations for inter-landmark distances included in PC2

	D14-D24	pr-D4	pt6-D4	D15-D25	pr-D5	pt4-D5	pt6-D5	D16-D26	pr-D6	pt4-D6	D17-D27	pr-D7	pt4-D7	pt6-D7
D14-D24	–													
pr-D4	0.613	–												
pt6-D4	0.682	0.254	–											
D15-D25	0.723	0.454	0.699	–										
pr-D5	0.684	0.761	0.617	0.705	–									
pt4-D5	0.666	0.366	0.758	0.966	0.651	–								
pt6-D5	0.678	0.431	0.699	0.985	0.690	0.945	–							
D16-D26	0.718	0.397	0.629	0.939	0.621	0.893	0.914	–						
pr-D6	0.686	0.735	0.637	0.665	0.958	0.592	0.682	0.624	–					
pt4-D6	0.591	0.232	0.870	0.878	0.607	0.907	0.878	0.876	0.622	–				
D17-D27	0.484	0.282	0.544	0.725	0.463	0.757	0.705	0.764	0.452	0.733	–			
pr-D7	0.645	0.654	0.587	0.621	0.840	0.560	0.639	0.612	0.904	0.592	0.588	–		
pt4-D7	0.427	0.179	0.766	0.726	0.496	0.762	0.747	0.721	0.528	0.876	0.830	0.672	–	
pt6-D7	0.473	0.237	0.543	0.726	0.422	0.745	0.723	0.768	0.433	0.738	0.972	0.619	0.882	–

Significant correlations ($p < 0.05$) are in **bold**.

PC 2

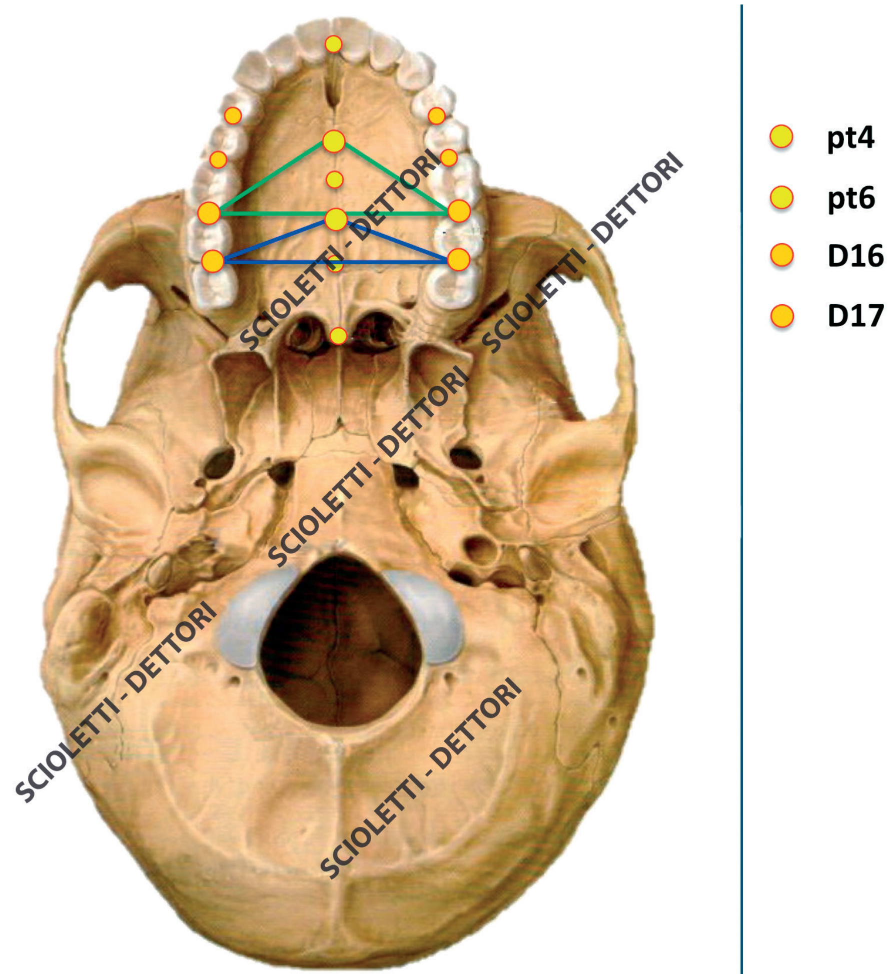

THE "UPPER CRANIUM SYSTEM"

The third component (PC3 - **11.13%**) showed positive correlations between the **zm**, bilateral zygomatic process, and midline maxillary inter-landmarks distances (**pr, pt4, pt5, pt6, pt7, sta**) and high negative loadings that include the **stl**, bilateral styloid process and the midline maxillary landmarks.

TABLE 6. Bivariate product-moment correlations for inter-landmark distances included in PC3

	zm-zm	pr-zm	pt4-zm	pt5-zm	pt6-zm	pt7-zm	sta-zm	stl-stl	pr-stl	pt4-stl	pt5-stl	pt6-stl	pt7-stl	sta-stl
zm-zm	–													
pr-zm	**0.955**	–												
pt4-zm	**0.946**	**0.966**	–											
pt5-zm	**0.944**	**0.953**	**0.975**	–										
pt6-zm	**0.966**	**0.947**	**0.964**	**0.987**	–									
pt7-zm	**0.965**	**0.921**	**0.935**	**0.950**	**0.980**	–								
sta-zm	**0.908**	**0.816**	**0.801**	**0.821**	**0.878**	**0.923**	–							
stl-stl	-0.275	-0.322	-0.213	-0.257	-0.300	-0.284	-0.249	–						
pr-stl	-0.187	-0.263	-0.222	-0.236	-0.207	-0.120	0.051	**0.556**	–					
pt4-stl	-0.220	-0.322	-0.229	-0.233	-0.225	-0.167	-0.036	**0.645**	**0.943**	–				
pt5-stl	-0.255	-0.354	-0.272	-0.263	-0.255	-0.204	-0.070	**0.648**	**0.935**	**0.988**	–			
pt6-stl	-0.245	-0.356	-0.284	-0.278	-0.257	-0.201	-0.053	**0.632**	**0.926**	**0.973**	**0.988**	–		
pt7-stl	-0.279	-0.389	-0.319	-0.321	-0.299	-0.241	-0.088	**0.666**	**0.918**	**0.964**	**0.973**	**0.990**	–	
sta-stl	-0.180	-0.210	-0.207	-0.169	-0.170	-0.159	-0.092	0.061	**0.400**	**0.406**	**0.486**	**0.460**	**0.385**	–

Significant correlations ($p < 0.05$) are in **bold**.

PC 3a

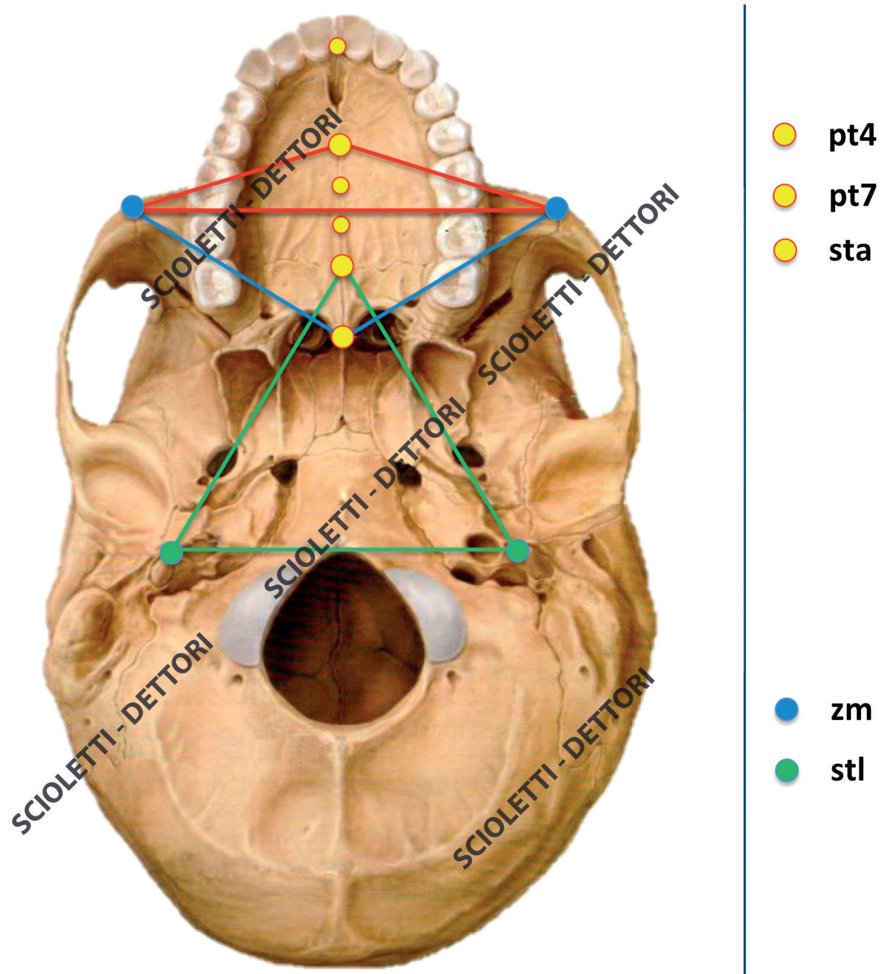

THE "UPPER CRANIUM SYSTEM"

Component three (PC3) (the "upper cranium system"), furthermore includes statistical correlations between the

nasion
base of sella turcica
zygomaxillare
opistiocranion

PC 3b

n, stb, zm and op landmarks (see Table 1 and Figure 1).

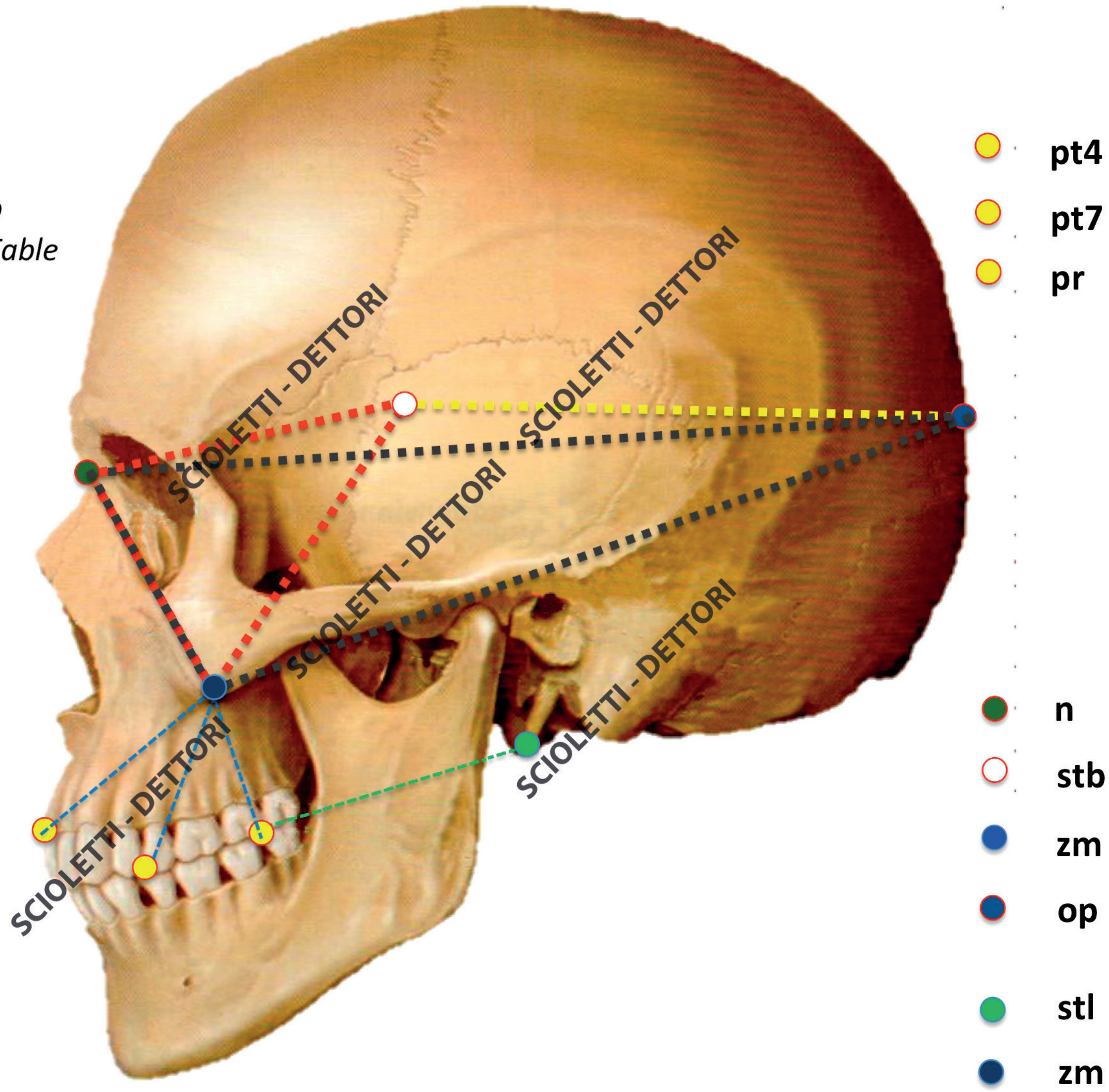

RESULTS

*The correlation between the lateral points (dental and facial) and the midline (***pr, ptz, ptg, sta, pht, bms***) of the skull seems to fit into the more general context of a symmetry that characterizes the whole human body.*

(Weyl 1952, Gardner 1990)

RESULTS

*The correlation between the dental and basal reference points located on the median line near the occipital hole (***pht, ba, o***) could provide new interesting information on the relationship between dental occlusal disturbances on the spine curvature (Ramirez-Yanez et al. Shimazaki et al., 2003).*

(Ramirez-Yanez et al. 2014; Shimazaki et al, 2003)

Geometric matrix

From our point of view, the correlations among new dental and cranial measurements shows the engram of the geometric matrix woven into skull architecture, following the evolutionary sequence of vascular-nervous tissues, Muscular t. Connective t. (cartilage and bone) in embryology…

… in the past several studies have been carried out on the relationship existing in human skull architecture, between bone triangles, dental triangles neural-vascular triangles (Ancon - Perù) (Sesimbra - Portugal) (Soacha, Cundinamarca - Colombia).

Simoes, A.W.

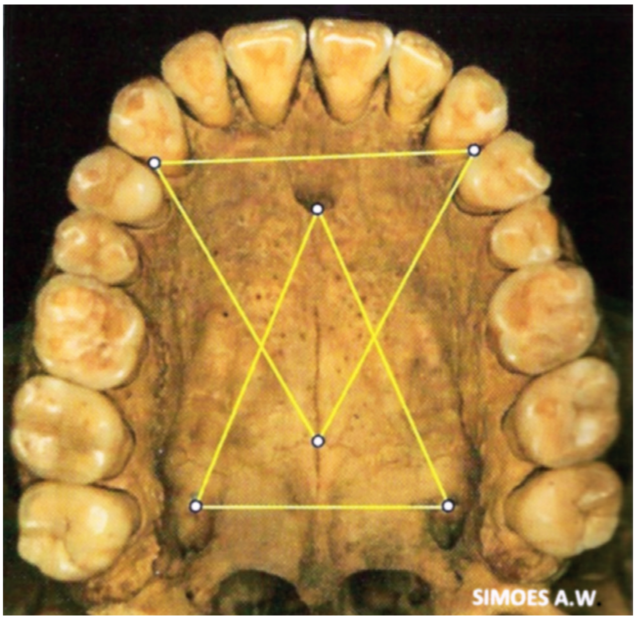

The presence of triangles tendentially equilateral and/or isoscopic are correlated to facial biotypology and the type of occlusion-mesio, disto or neutrocclusion.

Simoes A.W.

Galileo exposed in 1641 … the universe is written in mathematical language and the characters are triangles, squares, circles, spheres, cones and pyramids and other geometric figures without them it ‘s impossible to understand and understand nature …

THE GEOMETRICAL ANALYSIS OF THE ARCHITECTURE OF THE SKULL

The correlations on the geometry of skull architecture, shows that cranial development is subordinate to a mathematical code

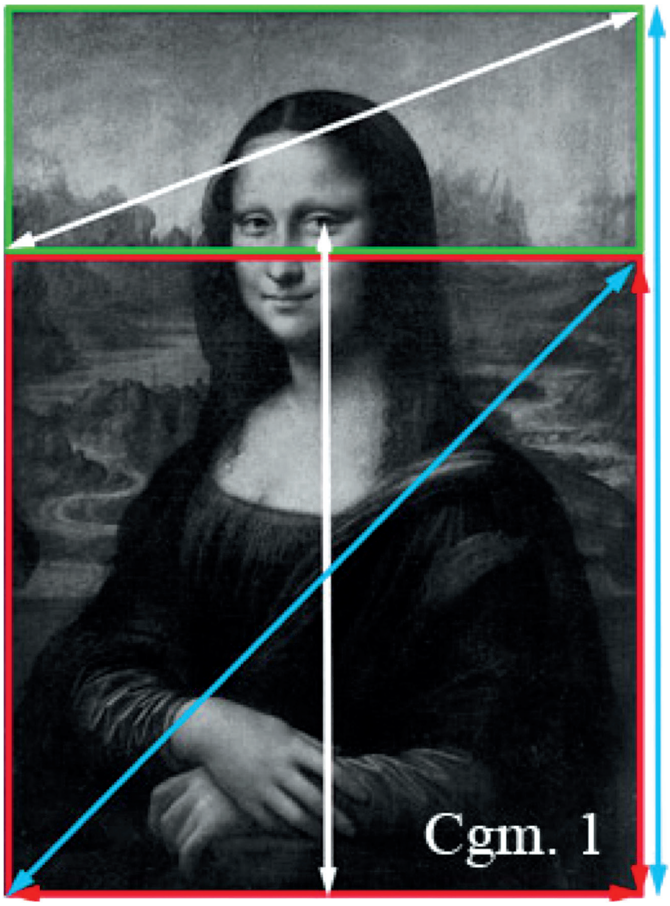

THE MATHEMATICAL CODE INCLUDES ALL THE LAWS OF NATURE

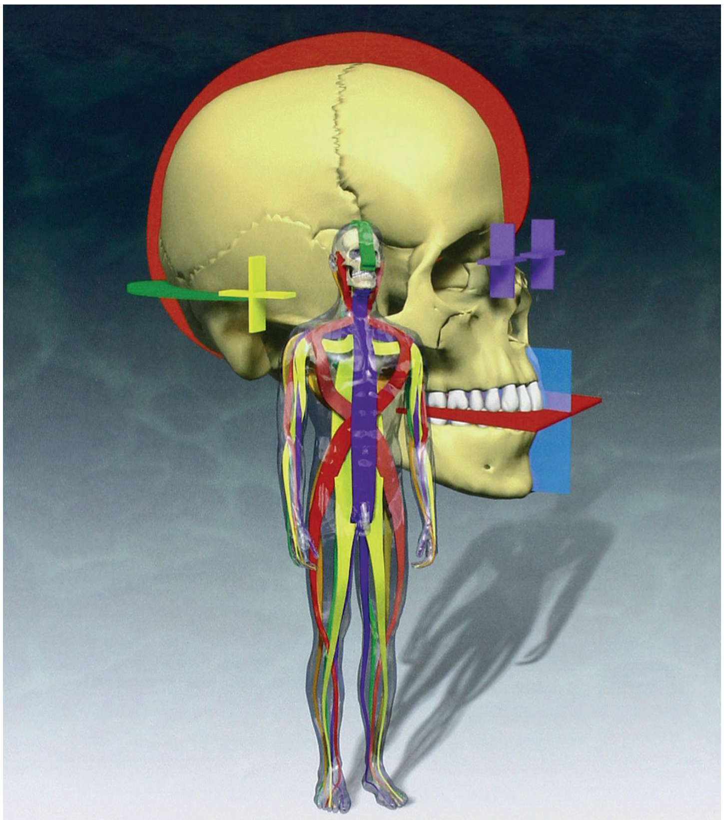

The theory of prime numbers and irrational numbers

$$2^{\frac{1}{2}} = \sqrt{2}$$

$$\pi \qquad \frac{-1 \pm \sqrt{5}}{2}$$

Symmetry

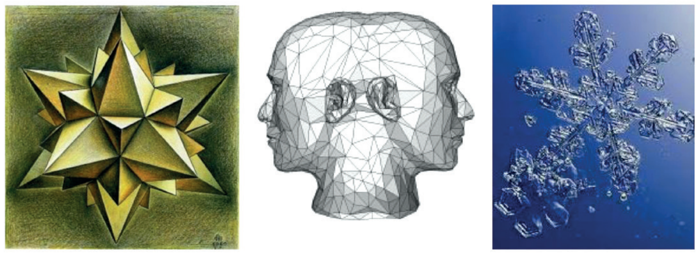

Proportionality golden section

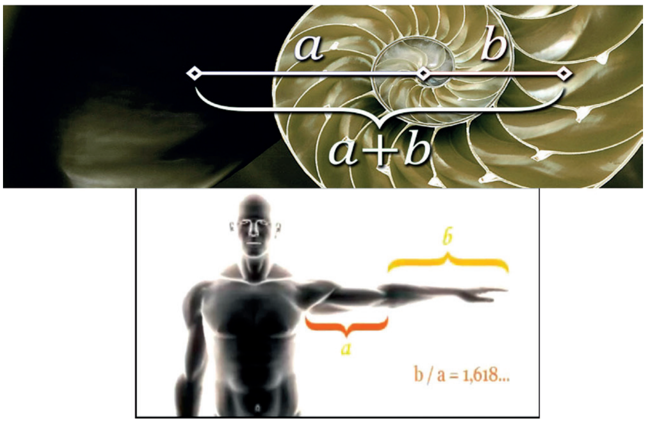

The laws of autosimilarity (*fratality*)

Orthogonality and sphericity

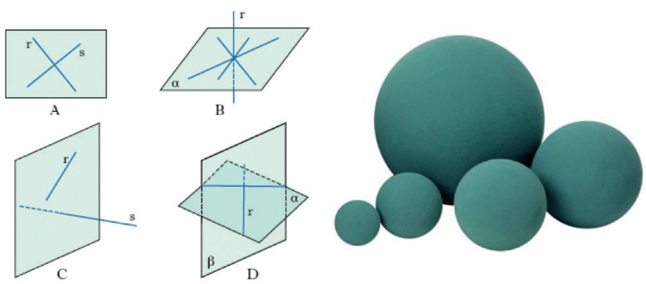

Equilibrium

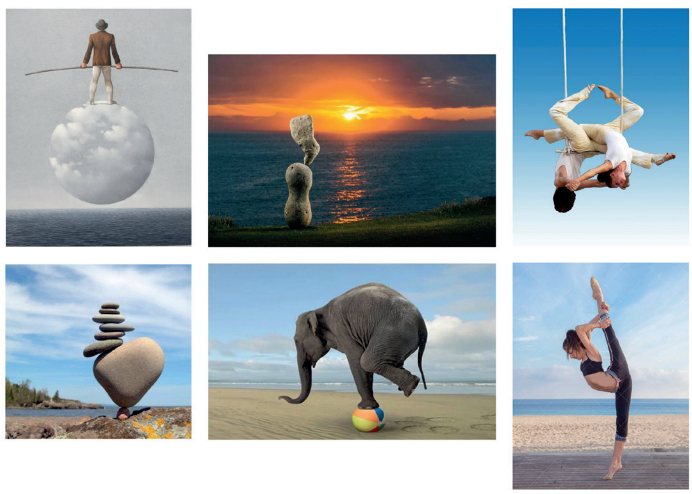

Gravity's force

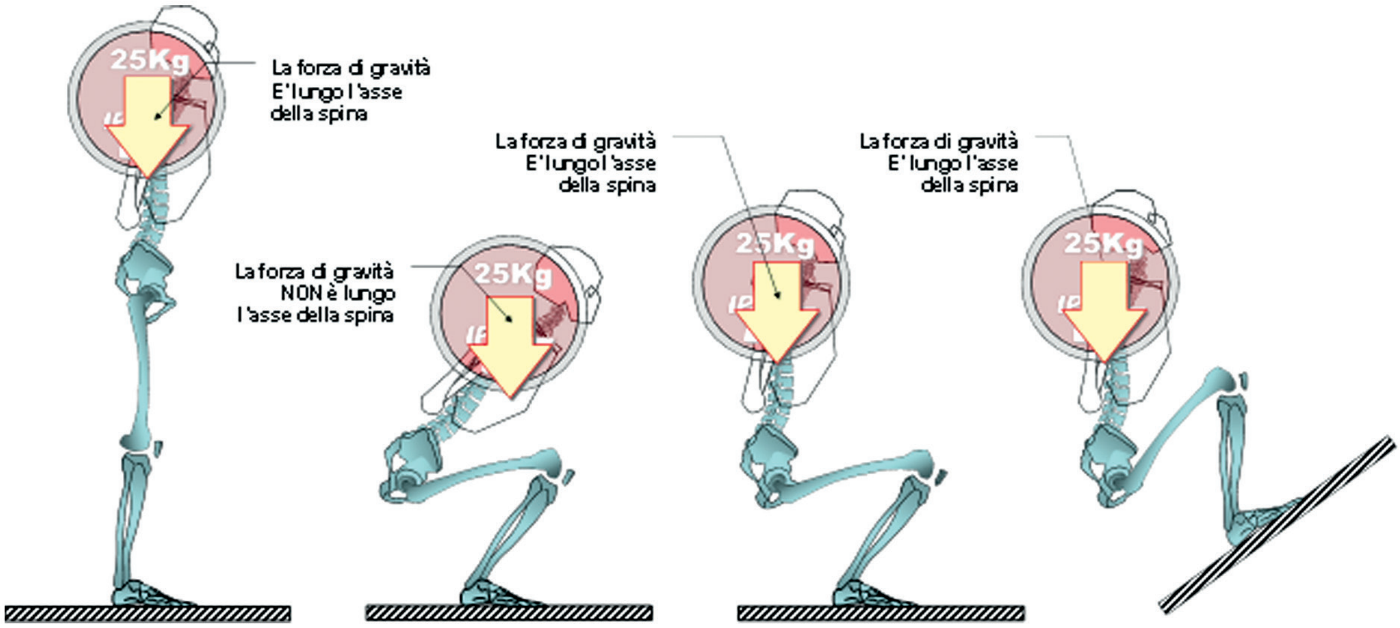

In physics the laws of gravitational phenomena are symmetrical in relation to rotations (direction changes).
The symmetry group of gravity law (the group of rotations in three-dimensional space) contains infinite elements related to rotation angles.

We can not' define the man or a part of it as the skull with a mathematical formula, but in this context we can use mathematical language to describe in general terms the relationship between the shape and size of the teeth and the architectural structure of the skull…

CONNESION NETWORK

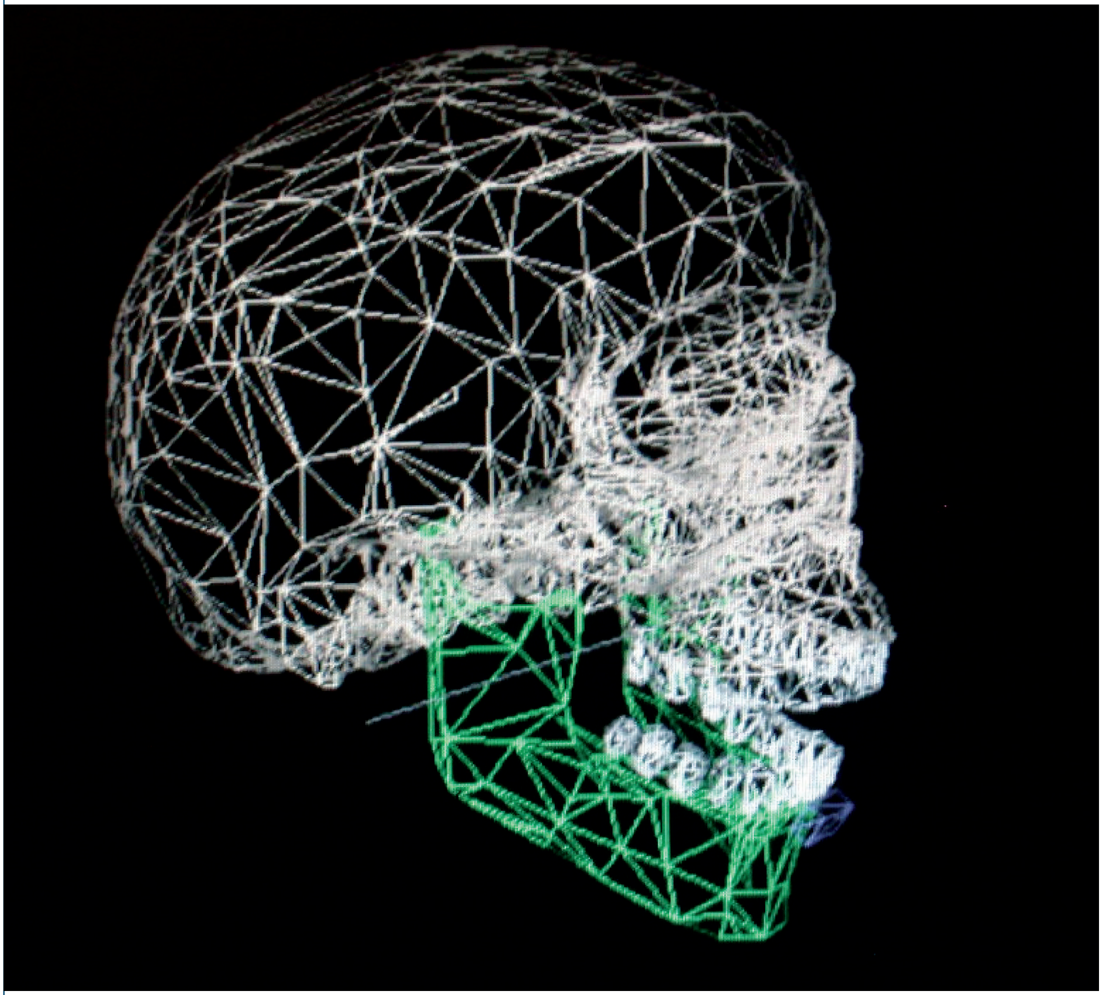

… we can consider the craniometric and dental landmarks analyzed in research as possible points of the connection network, releated to our wole body and to everyhing in around us…

… maby there is a correlation that will probably be demonstrated in the future between the crystalline or almost crystalline nature of living matter and the topology of the networks connections that emerge …